

Native geometry and the dynamics of protein folding

P. F. N. Faisca and M. M. Telo da Gama^{1,*}

¹*CFTC, Av. Prof. Gama Pinto 2, 1649-003 Lisboa Codex, Portugal*

(Dated: November 21, 2018)

Abstract

In this paper we investigate the role of native geometry on the kinetics of protein folding based on simple lattice models and Monte Carlo simulations. Results obtained within the scope of the Miyazawa-Jernigan indicate the existence of two dynamical folding regimes depending on the protein chain length. For chains larger than 80 amino acids the folding performance is sensitive to the native state's conformation. Smaller chains, with less than 80 amino acids, fold via two-state kinetics and exhibit a significant correlation between the contact order parameter and the logarithmic folding times. In particular, chains with $N=48$ amino acids were found to belong to two broad classes of folding, characterized by different cooperativity, depending on the contact order parameter. Preliminary results based on the $G\bar{o}$ model show that the effect of long range contact interaction strength in the folding kinetics is largely dependent on the native state's geometry.

PACS numbers: 87.15.Cc; 91.15.Ty

Keywords: protein folding, lattice models, contact order, long-range contacts, kinetics, cooperativity

INTRODUCTION

It is well known that most small (from ~ 50 -120 amino acids), single domain proteins fold via a two-state (single exponential) kinetics, without observable folding intermediates and with a single transition state associated with one major free energy barrier separating the native state from the unfolded conformations [1, 2, 3]. For this reason small protein molecules are particularly well suited for investigating the correlations between folding times and the native state equilibrium properties, a major challenge for those working in protein research.

The energy landscape theory predicts that the landscape’s ruggedness plays a fundamental role in the folding kinetics of model proteins: The existence of local energy minima, that act as kinetic traps, is responsible for the overall slow and, under some conditions (as the temperature is lowered towards the glass transition temperature), glassy dynamics [4]. On the other hand, rapid folding is associated with the existence of a smooth, funnel-shaped energy landscape [5]. In Refs. [6, 7] Plaxco *et. al.* and Gillespie and Plaxco have provided experimental evidence that the folding energy landscape of single domain proteins is extremely smooth even at considerably low temperatures. Therefore differences in the landscape’s ‘topography’ cannot account for the vast range of folding rates as observed in real proteins [8, 9]. However, a strong correlation ($r=0.94$) was found between the so-called contact order parameter, CO, and the experimentally observed folding rates in a set of 24 non-homologous single domain proteins [10]. The CO measures the average sequence separation of contacting residue pairs in the native structure relative to the chain length of the protein

$$CO = \frac{1}{LN} \sum_{i,j}^N \Delta_{i,j} |i - j|, \quad (1)$$

where $\Delta_{i,j} = 1$ if residues i and j are in contact and is 0 otherwise; N is the total number of contacts and L is the protein chain length. The empirical observation that the CO correlates well with the folding rates of single domain proteins, exhibiting smooth energy landscapes, strongly suggests a geometry-dependent kinetics for such two-state folders.

The connection between the CO and the dominant range of residue interactions brings back an old, well-debated issue in the protein folding literature, that of the role of local (i.e. close in space and in sequence) and long range (i.e. close in space but distant along the sequence) inter-residue interactions in the folding dynamics. Several results appear to agree on the idea that long range (LR) contacts play an active role in stabilizing the native fold

[11, 12, 13, 14]. In what regards the folding kinetics, results reported in Refs. [11, 13, 15, 16] suggest that local contacts increase the folding speed, relative to LR contacts, while results in Ref. [12] suggest an opposite trend. In Ref. [17] Gromiha and Selvaraj have analysed explicitly the contribution of LR contacts in determining the folding rates of 23 (out of the 24) two-state folders studied by Plaxco *et al* [10]. These authors proposed the so-called long range order (LRO) parameter, measuring the total number of long range contacts relative to the protein chain length, as an alternative way of quantifying the native structure geometry. In fact, the LRO parameter correlates as well as the CO with the folding rates of the two-state folders analysed in Ref. [10].

The majority of protein folding theory is based, not only on results for real proteins such as those outlined above, but also on a vast number of findings obtained within the scope of simple lattice models and Monte Carlo (MC) simulations. Although lattice models do not encompass the full complexity of real proteins they are non trivial and capture fundamental aspects of the protein folding kinetics [18].

In the present study we investigate through Monte Carlo folding simulations of simple lattice models, such as the Miyazawa-Jernigan model and the Gō model, the dependence of two-state folding kinetics on the native state geometry.

LATTICE MODELS

In a lattice model the protein is reduced to its backbone structure: amino acids are represented by beads of uniform size, occupying the lattice vertices, and the peptide bond, that covalently connects amino acids along the polypeptide chain, is represented by sticks, with uniform length, corresponding to the lattice spacing. We model proteins as three-dimensional, self-avoiding chains of N beads. To mimick amino acid interactions we use either the Miyazawa-Jernigan model or the Gō model.

The Miyazawa-Jernigan model

In the Miyazawa-Jernigan (MJ) model the energy of a conformation defined by the set of bead coordinates $\{\vec{r}_i\}$ is given by the contact Hamiltonian

$$H(\{\sigma_i\}, \{\vec{r}_i\}) = \sum_{i>j}^N \epsilon(\sigma_i, \sigma_j) \Delta(\vec{r}_i - \vec{r}_j), \quad (2)$$

where $\{\sigma_i\}$ represents an amino acid sequence, and σ_i stands for the chemical identity of bead i . The contact function Δ is 1 if beads i and j are in contact but not covalently linked and is 0 otherwise. The interaction parameters ϵ are taken from the 20×20 MJ matrix, derived from the distribution of contacts of native proteins [19].

The G \bar{o} model

In the G \bar{o} [11] model only native contacts, i.e. contacts that are present in the native state, contribute to the energy of a conformation defined by $\{\vec{r}_i\}$. In this case the contact Hamiltonian is

$$H(\{\vec{r}_i\}) = \sum_{i>j}^N B_{ij} \Delta(\vec{r}_i - \vec{r}_j), \quad (3)$$

where the contact function $\Delta(\vec{r}_i - \vec{r}_j)$, is unity only if beads i and j form a non-covalent native contact and is zero otherwise. Since the G \bar{o} model ignores the protein sequence chemical composition the interaction energy parameter is $B_{ij} = -\epsilon$.

SIMULATION DETAILS

Our folding simulations follow the standard MC Metropolis algorithm [20] and, in order to mimick protein movement, we use the kink-jump move set, including corner flips, end and null moves as well as crankshafts [21].

Each MC run starts from a randomly generated unfolded conformation (typically with less than 10 native contacts) and the folding dynamics is traced by following the evolution of the fraction of native contacts, $Q = q/Q_{max}$, where Q_{max} is the total number of native contacts and q is the number of native contacts at each MC step. The folding time t , is taken as the first passage time (FPT), that is, the number of MC steps corresponding to $Q = 1.0$.

The folding dynamics is studied at the so-called optimal folding temperature, the temperature that minimizes the folding time as measured by the mean FPT.

The sequences studied within the context of the MJ model were prepared by using the design method developed by Shakhnovich and Gutin (SG) [22] based on random heteropolymer theory and simulated annealing techniques. All targets studied are maximally compact structures found by homopolymer relaxation.

NUMERICAL RESULTS

Evidence for two folding regimes in protein folding

Figure 1(a) shows the dependence on time t , of the folding probability $P_{fold}(t)$, for chain lengths $N = 27, 36, 48, 54, 64, 80, 100$. Five target structures were considered per chain length and thirty SG sequences were prepared according to the method described in Ref. [22].

$P_{fold}(t)$, the probability of the chain having visited its target after time t , was computed as the fraction of (150) simulation runs, which ended at time t . Two distinct folding regimes were identified depending on the chain length. We name the regime observed for $N < 80$ the *first regime* while that corresponding to $N \geq 80$ is the *second regime*. We have investigated the contribution of each target to the folding probability curve and found that for $N \geq 80$ the folding performance is sensitive to target conformation, with some targets being more foldable than others as shown in Figure 1(b) for $N=100$. For $N < 80$ targets are equally foldable since all folding probability curves are consistent with asymptotic values $P_{fold} \rightarrow 1$.

In order to investigate if kinetic relaxation in the first regime is well described by a single exponential law we have calculated the dependence of $\ln(1 - P_{fold})$ on the time coordinate t . Remember that in a two-state process the reactant concentration (the equivalent in our simulations to the fraction of unfolded chains) is proportional to $\exp^{-t/\tau}$ where τ is the so-called relaxation time. Therefore, if first regime kinetics is single exponential $\ln(1 - P_{fold})$ vs. t should be a straight line with slope $= -1/\tau$. Results reported in Figure 2 show that single-exponential folding is indeed a very good approximation for the folding kinetics of small lattice-polymer proteins.

Contact order and the lattice-polymer model kinetics

In a recent study [24] we analysed the folding kinetics of ≈ 5000 SG sequences and 100 target conformations distributed over the chain lengths $N = 36, 48, 54, 64$ and 80. Targets were selected in order to cover the observed range of CO ($\approx 0.12 < \text{CO} < 0.26$). Results reported in Ref. [24] show a significant correlation ($r = 0.70 - 0.79$) between increasing CO and longer logarithmic folding times. In Ref. [25] Jewett *et al.* found a similar correlation ($r = 0.75$) for a 27-mer lattice polymer modeled by a modified G \bar{o} -type potential. In a recent study, Kaya and Chan [26] studied a modified G \bar{o} type model, with specific many-body interactions, and found folding rates that are very well correlated ($r = 0.91$) with the CO and span a range that is two orders of magnitude larger than that of the corresponding G \bar{o} models with additive contact energies. These results support the empirical relation found between the contact order and the kinetics of two-state folders.

Contact order and structural changes towards the native fold in the Miyazawa-Jernigan model

In order to investigate if native geometry as measured by the CO promotes, or does not promote, different folding processes, eventually leading to different folding rates, we have analysed the dynamics of 900 SG sequences with chain length $N = 48$, distributed over nine target structures with low (0.126, 0.127, 0.135), intermediate (0.163, 0.173, 0.189) and high (0.241, 0.254, 0.259) contact order. The averaged trained sequence energy shows very little dispersion ranging from -25.11 ± 0.03 to -26.16 ± 0.02 . Within this target set the folding time and the contact order correlate well ($r = 0.82$) although the dispersion of folding times is small as reported in Figure 3.

The contact map is a $N \times N$ matrix with entries $C_{ij} = 1$ if beads i and j are in contact (but not covalently linked) and are zero otherwise. Figure 4 shows the contact maps of targets T1 (CO=0.126), T2 (CO=0.189) and T3 (CO=0.259) respectively. One could argue that high-CO targets are associated with longer logarithmic folding times because they have predominantly LR contacts which, given the local nature of the move set used to simulate protein movement, eventually take a longer time to form. Let the contact time t_0 be the mean FPT of a given contact averaged over 100 MC runs. The longest contact

time ($\ln t_0 = 12.24$) observed for target T3 is two orders of magnitude shorter than T3's folding time ($\ln t = 17.59$) and the sum of all contact times is $\ln(\sum_{i=1}^{57} t_0^i) = 15.51$, much lower than the observed folding time. Thus, the fact that T3 and other high-CO structures have predominantly LR contacts cannot justify, *per se*, their higher folding times.

The contact map provides a straightforward way to compute the frequency $\omega_{ij} = t_{ij}/t$ with which a native contact occurs in a MC run, t_{ij} being the number of MC steps corresponding to $C_{ij} = 1$ and t the folding time. For each target studied we computed the mean frequency of each native contact $\langle \omega_{ij} \rangle$ averaged over 100 simulation runs, and re-averaged $\langle \omega_{ij} \rangle$ over the number of native contacts in each interval of backbone distance (we measure backbone distance in units of backbone spacing). We have found that while for the low-CO targets the backbone frequency decreases monotonically with increasing backbone distance, for the intermediate and high-CO targets such dependence is clearly nonmonotonic. Figure 5 illustrates this behaviour for model structures T1, T2 and T3 elements of the low, intermediate and high-CO target sets respectively. A possible explanation for this behavior, that we have ruled out, is that of a negative correlation between the frequency and the energy of a contact; Could the most stable contacts be the most frequent ones? We found modest correlation coefficients $r = 0.63$ and $r = 0.65$ for targets T1 and T3 respectively and therefore we conclude that the observed behaviour is not energy driven.

In Table I we show the dependence of the contact time, averaged over contacts in each interval of backbone distance, on the backbone distance for model targets T1 and T3. Since the average contact times, over a given range, are similar for these extreme model structures, the differences in the frequencies reported in Figure 5 must necessarily distinguish different cooperative behaviors.

Results outlined above suggest that two broad classes of folding mechanisms exist for small MJ lattice polymer protein chains. What distinguishes these two classes is the presence, or absence, of a monotonic decrease of contact frequency with increasing contact range that is related to different types of cooperative behaviour. The monotonic decrease of contact frequency with increasing backbone distance is a specific trait of low-CO structures. In this case folding is also less cooperative and is driven by backbone distance: Local contacts form first while LR contacts form progressively later as contact range increases.

Contact order, long-range contacts and protein folding kinetics in the G \bar{o} model

The energy landscapes of G \bar{o} -type polymers are considerably smooth because in the G \bar{o} model the only favourable interactions are those present in the native state. Therefore such models are adequate for investigating the dependence of protein folding kinetics on target geometry.

In this section we investigate the contribution of LR and local interactions to the folding kinetics of targets T1, T2 and T3 (Figure 4) in the following way: The total energy of the native structure is kept constant but the relative contributions of LR and local interactions are varied over a broad range. With the above constraint the energy of a conformation is given by

$$H(\{\vec{r}_i\}, \sigma) = C_{LR}(\sigma)H_{LR}(\{\vec{r}_i\}) + C_L(\sigma)H_L(\{\vec{r}_i\}), \quad (4)$$

where $C_{LR}(\sigma) = \sigma/[(1-\sigma)Q_L + \sigma(1-Q_L)]$ and $C_L(\sigma) = (1-\sigma)/[(1-\sigma)Q_L + \sigma(1-Q_L)]$; Q_L is the fraction of local native contacts and $H_{LR}(L)$ is given by equation 3. The parameter σ varies from 0 (only local contacts contribute to the total energy) to 1 (only LR contacts contribute to the total energy).

The constraint of fixed native state energy is enforced to rule out differences in the folding dynamics driven by the stability of the native state.

Preliminary results reported in Figure 6 show the dependence of the logarithmic folding time, averaged over 100 simulations runs, on the parameter σ for the three native geometries. For $\sigma < 0.15$ we have not observed folding of the target T3 and no folding was observed for the target T2 if $\sigma < 0.10$.

The behaviour exhibited by target T3 is easily explained: since approximately 80 percent of T3's native contacts are LR there is little competition between LR and local contacts. Moreover, such competition is not significantly enhanced when one varies σ towards unity. However, the effect of decreasing σ is equivalent to that of 'switching off' the LR contacts, that is, to force a structure to fold with only approximately 20 per cent of its total native contacts resulting in longer folding times and for $\sigma < 0.15$ folding failure. More intriguing are the results obtained for the low and intermediate-CO target structures, T1 and T2 respectively. The curves are qualitatively similar (with a minimum at $\sigma > 0.5$) but closer inspection reveals an important difference, namely: for $\sigma < 0.5$ the dependence of the folding time on σ is much stronger for the intermediate-CO target, T2. Indeed, in this

case one observes a remarkable three-order of magnitude dispersion of logarithmic folding times, ranging from $\log(t) = 5.62$ (for $\sigma = 0.65$) to $\log(t) = 8.50$ (for $\sigma = 0.10$). We stress, however, that for both targets the kinetics is more sensitive (in the sense that the folding rate decreases more rapidly) to lowering σ : LR contacts appear therefore to have a crucial/vital role, by comparison with local contacts, in determining the folding rates of small G \bar{o} -type lattice polymers and this effect depends on target geometry.

CONCLUSIONS AND FINAL REMARKS

By using different target structures in MC simulations of protein folding we have identified two distinct folding regimes depending on the chain length. In close agreement with experimental observations we found a first regime that describes well the folding of small protein molecules and whose kinetics is single exponential. Folding of protein chains with more than 80 amino acids, on the other hand, belongs to a dynamical regime that appears to be target sensitive with some targets being more highly foldable than others. In this case we ascribe folding failure to existing kinetic traps but we have not been able to carry out our simulations for long enough times in order to observe escape and successful folding.

Because the additive MJ lattice polymer model fails to exhibit the remarkable dispersion of folding rates observed in real proteins one should interpret the results for the dependence of folding times on contact order parameter with caution. However, our results strongly suggest that the geometry driven cooperativity is rather robust and this implies an increase in folding times for increasing cooperativity.

We have analysed the role of LR contacts in the folding kinetics of small G \bar{o} -type lattice polymers and found a considerably strong dependence on target geometry. In particular, we have found that targets with a similar fraction of LR contacts (that is, targets with similar LRO parameter) and different contact order exhibit considerably different folding rates when LR contacts are destabilized energetically with respect to local contacts. We are currently investigating this issue and results will be published elsewhere (in preparation). This result may provide a clue to understanding the incredible dispersion of folding rates exhibited by real two-state folders: one can expect to observe longer folding times if the distribution of contact energies in real proteins is such that local contacts are, on average, more stable than LR contacts for specific native folds.

ACKNOWLEDGEMENTS

P.F.N.F. would like to thank Fundação para a Ciência e Tecnologia for financial support through grant No. BPD10083/2002.

* Electronic address: patnev@alf1.cii.fc.ul.pt

- [1] S. E. Jackson, How do small protein molecules fold?, *Folding Des.* 3 (1998) 81-91
- [2] K. W. Plaxco, K. T. Simmons and D. Baker, Contact order, transition state placement and the refolding rates of single domain proteins, *J. Mol. Biol.* 277 (1998) 985-994
- [3] H. Kaya and H. S. Chan, Simple two-state protein folding kinetics requires near-levinthal thermodynamic cooperativity, *Proteins* 52 (2003) 510-523
- [4] J. D. Bryngelson and P. G. Wolynes, Spin glasses and the statistical mechanics of protein folding, *Proc. Natl. Acad. Sci. U.S.A.* 84 (1987) 7524-7528
- [5] P. E. Leopold, M. Montal and J. N. Onuchic, Protein folding funnels - a kinetic approach to the sequence structure relationship, *Proc. Natl. Acad. Sci. U.S.A.* 89 (1992) 8721-8725
- [6] K. W. Plaxco, I. S. Millet, D. J. Segel, S. Doniach and D. Baker, Polypeptide chain collapse can occur concomitantly with the rate limiting step in protein folding, *Nat. Struct. Biol.* 6 (1999) 554-557
- [7] B. Gillespie and K. W. Plaxco, Non-glassy kinetics in the folding of a simple single domain protein, *Proc. Natl. Acad. Sci. U.S.A.* 97 (2000) 12014-12019
- [8] P. Wittung-Stafshede, J. C. Lee, J. R. Winkler and H. B. Gray, Cytochrome b(562) folding triggered by electron transfer: Approaching the speed limit for formation of a four-helix-bundle protein, *Proc. Natl. Acad. Sci. USA* 96 (1999) 6587-6590
- [9] N. A. J. van Nuland, F. Chiti, N. Taddei, G. Raugei, G. Ramponi and C. M. Dobson, Slow folding of muscle acylphosphatase in the absence of intermediates, *J. Mol. Biol.* 283 (1998) 883-891
- [10] K. W. Plaxco, K. T. Simmons, I. Ruczinski and D. Baker, Topology, stability, sequence, and length: Defining the determinants of two-state protein folding kinetics *Biochemistry* 39 (2000) 11177-11183

- [11] N. Gō and H. Taketomi, Respective role of short- and long-range interactions in protein folding, Proc. Natl. Acad. Sci. U.S.A. 75 (1978) 559-563
- [12] V. I. Abkevich, A. M. Gutin and E. I. Shakhnovich, Impact of local and non-local interactions on thermodynamics and kinetics of protein folding, J. Mol. Biol. 252 (1995) 460-471
- [13] Doyle R., Simmons K. Qian H. and Baker D., Local interactions and the optimization of protein folding, Proteins 29 (1997) 282-291
- [14] M. M. Gromiha and S. Selvaraj, Importance of long-range interactions in protein folding, Biophys. Chem. 77 (1999) 49-68
- [15] D. B. Wetlaufer, Nucleation, rapid folding, and globular intrachain regions in proteins, Proc. Natl. Acad. Sci. U.S.A. 70 (1973) 697-701
- [16] R. Unger and J. Moult, Local Interactions dominate folding in a simple lattice protein model, J. Mol. Biol. 259 (1996) 988-994
- [17] M. M. Gromiha and S. Selvaraj, Comparison between long-range interactions and contact order in determining the folding rate of two-state proteins: application of long-range order to folding prediction, J. Mol. Biol. 310 (2001) 27-32
- [18] L. Mirny and E. I. Shakhnovich in: Protein folding evolution and design, Proceedings of the International School of Physics Enrico Fermi, Course CXLV, edited by R. A. Broglia and E. I. Shakhnovich, IOS Press, Ohmsha (2001), p. 38
- [19] S. Miyazawa and R. L. Jernigan, Estimation of effective interresidue contact energies from protein crystal-structures-quasi-chemical approximation, Macromolecules 18 (1985) 534-552
- [20] N. Metropolis, A. W. Rosenbluth, M. N. Rosenbluth, A. H. Teller and E. Teller, Equation of state calculations by fast computing machines, J. Chem. Phys. 21 (1953) 1087-1092
- [21] D. P. Landau and K. Binder, A Guide to Monte Carlo Simulations in Statistical Physics (Cambridge University Press, 2000)
- [22] E. I. Shakhnovich and A. M. Gutin, Engineering of stable and fast-folding sequences of model proteins, Proc. Natl. Acad. Sci. U.S.A. 90 (1993) 7195-7199
- [23] P. F. N. Faisca and R. C. Ball, Thermodynamic control and dynamical regimes in protein folding, J. Chem. Phys. 116 (2002) 7231-7238
- [24] P. F. N. Faisca and R. C. Ball, Topological complexity, contact order and protein folding rates, J. Chem. Phys. 117 (2002) 8587-8591

- [25] A. I. Jewett, V. S. Pande and K. W. Plaxco, Cooperativity, smooth energy landscapes and the origins of topology-dependent kinetics protein folding rates, *J. Mol. Biol.* 326 (2003), 247-253
- [26] H. Kaya and H. S. Chan, Contact order dependent protein folding rates: Kinetic consequences of a cooperative interplay between favorable nonlocal interactions and local conformational preferences, *Proteins* 52 (2003) 524-533
- [27] P. F. N. Faisca, M. M. Telo da Gama and R. C. Ball, Folding and form: Insights from lattice simulations, *Phys. Rev. E* 69 (2004) 051917

FIGURES

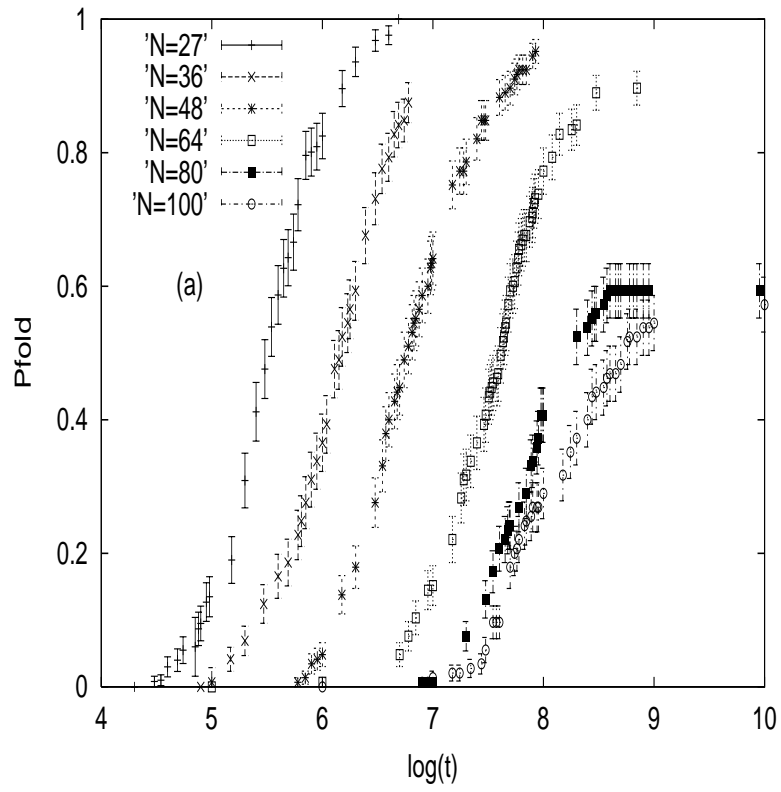


Figure 1(a); P.N.F. Faisca, Biophysical Chemistry

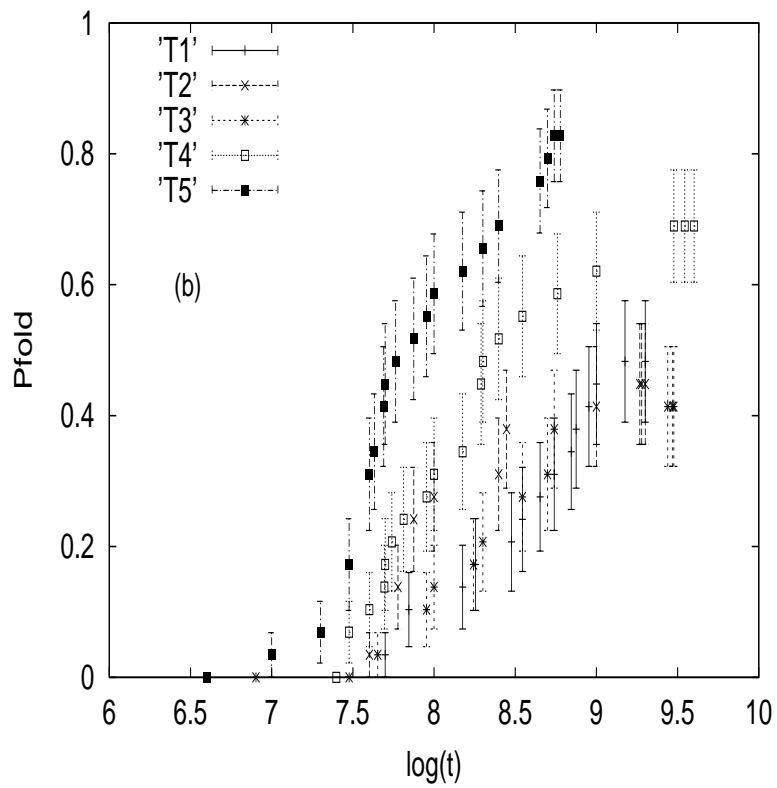


Figure 1(b); P.N.F. Faisca, Biophysical Chemistry

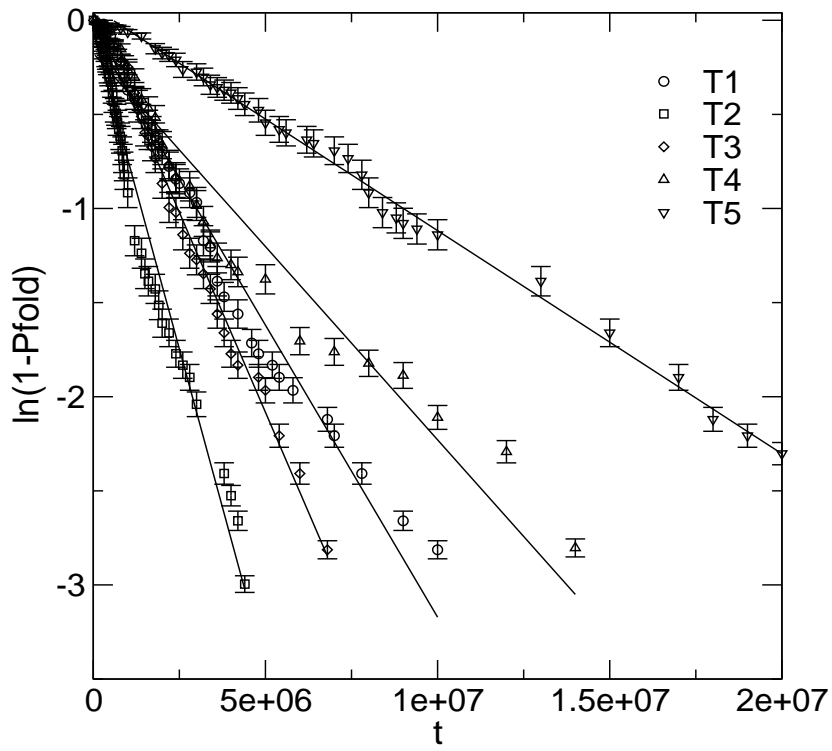


Figure 2; P.N.F. Faisca, Biophysical Chemistry

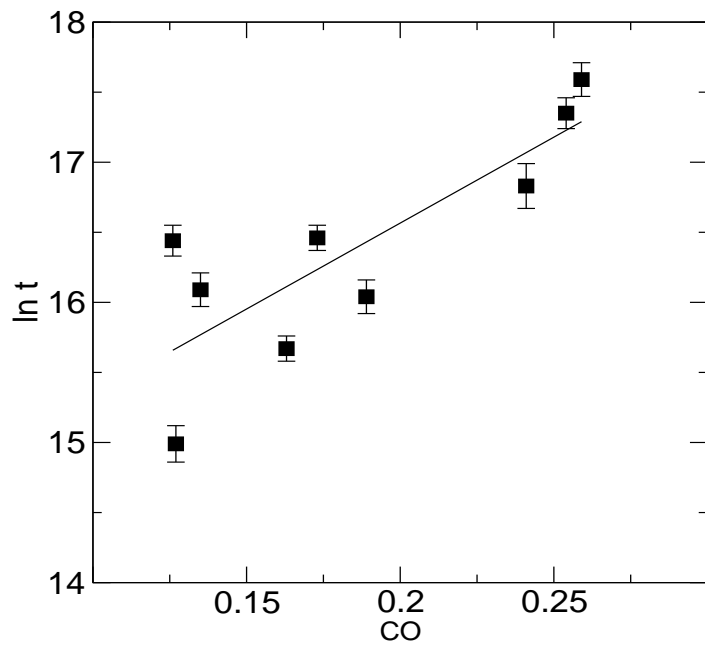


Figure 3; P.N.F. Faisca, Biophysical Chemistry

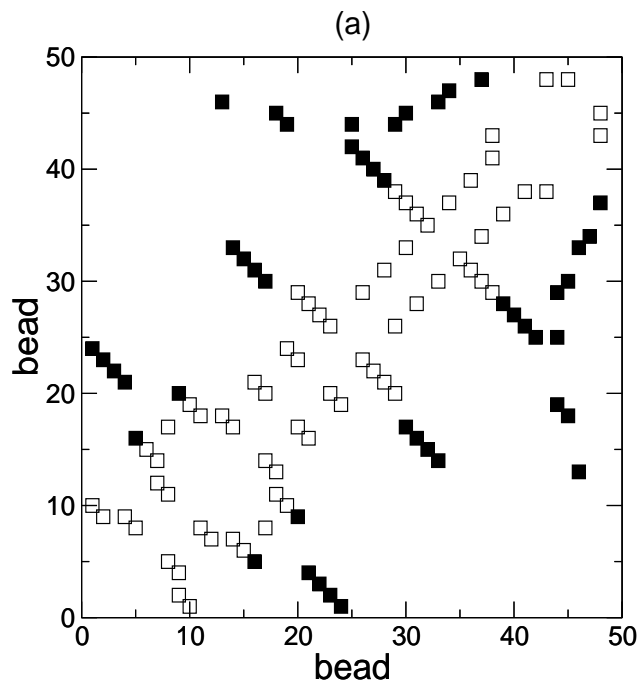


Figure 4(a); P.N.F. Faisca, Biophysical Chemistry

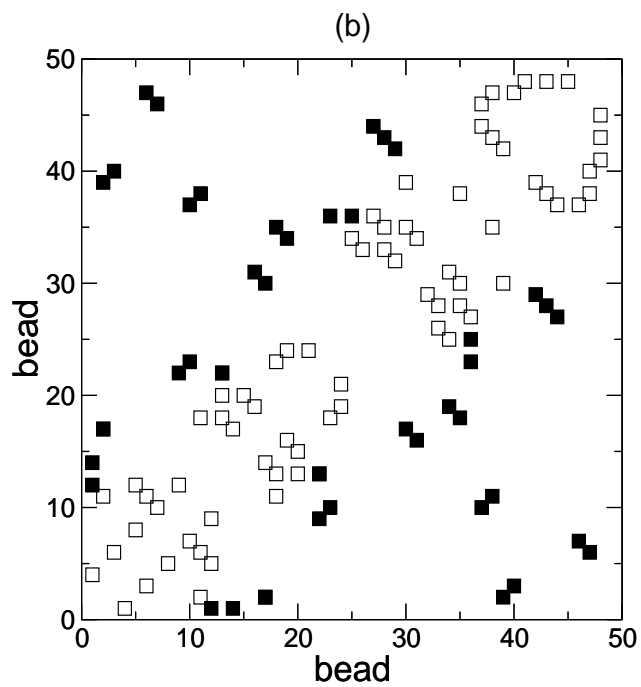


Figure 4(b); P.N.F. Faisca, Biophysical Chemistry

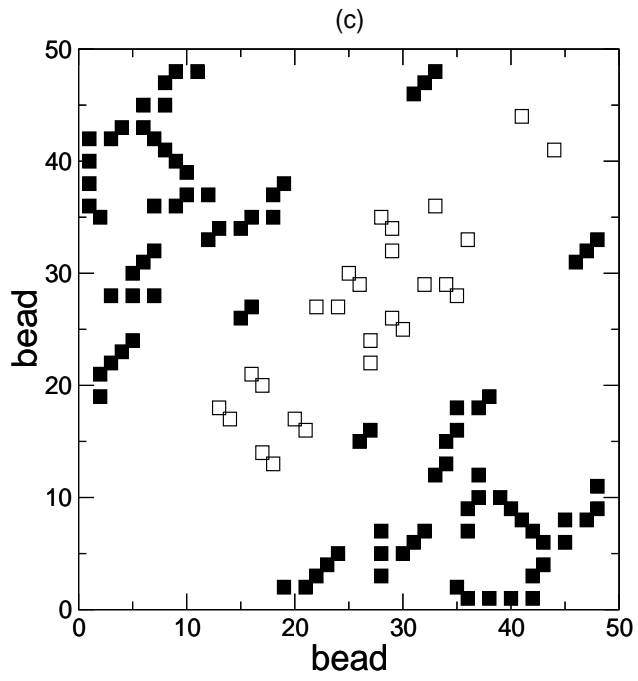


Figure 4(c); P.N.F. Faisca, Biophysical Chemistry

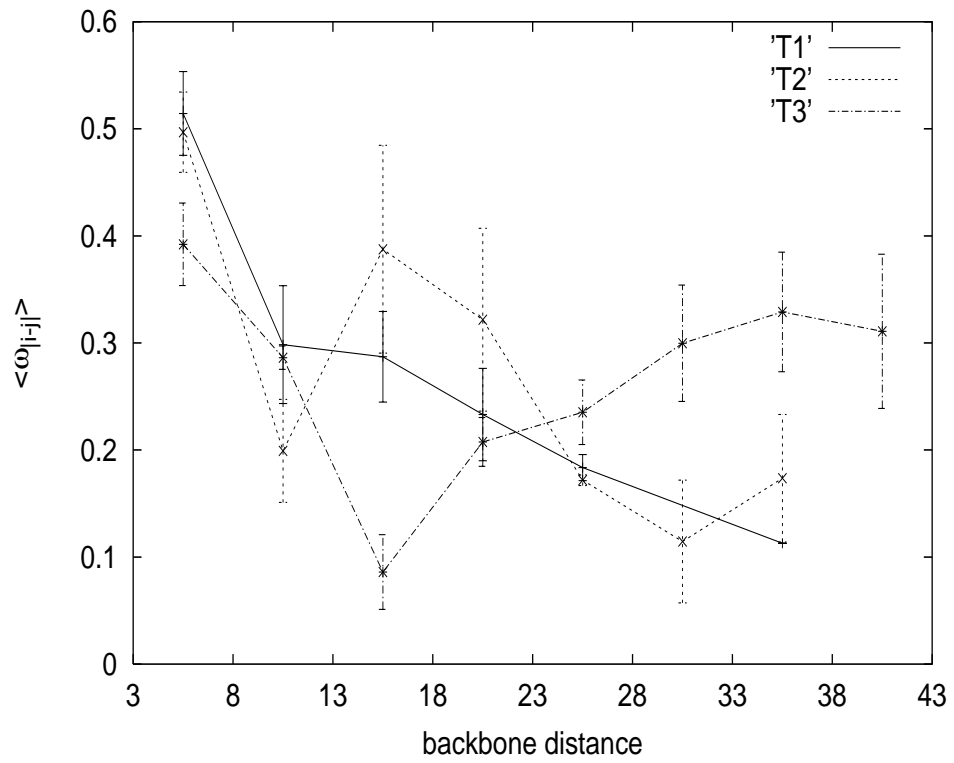


Figure 5; P.N.F. Faisca, Biophysical Chemistry

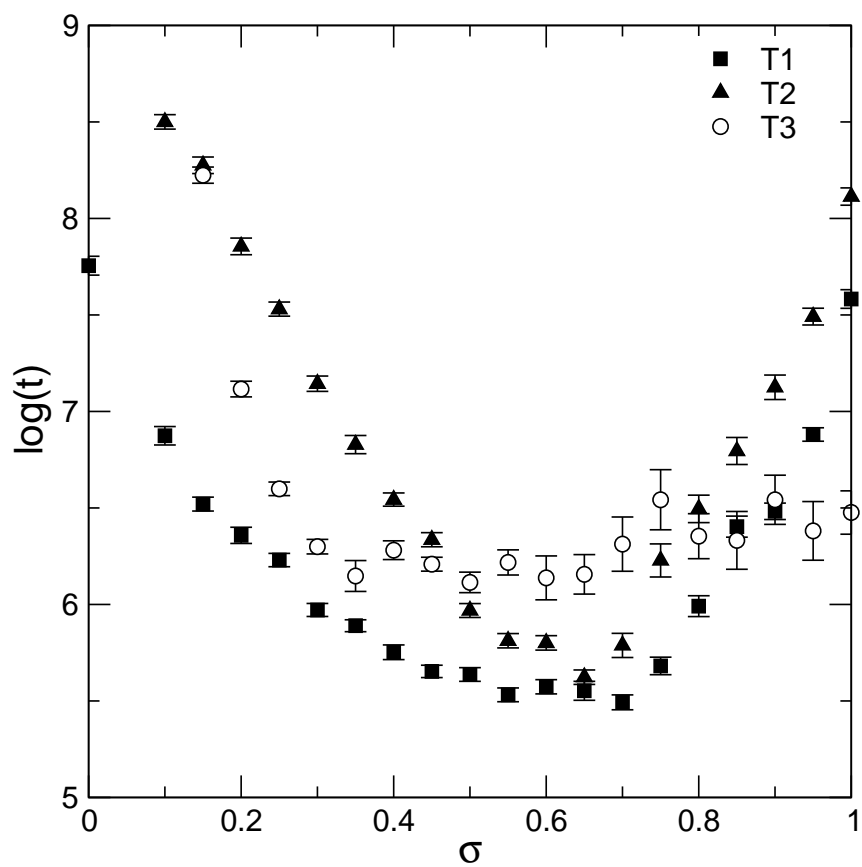


Figure 6; P.N.F. Faisca, Biophysical Chemistry

FIGURE CAPTIONS

Figure 1. Dependence of the folding probability, P_{fold} , on $\log(t)$. (a) For each of the chain lengths $N = 27, 36, 48, 64, 80$ and 100 five target structures were considered and 30 sequences were designed per target. P_{fold} , the probability of the chain having visited its target after time t , was computed as the fraction of simulation runs that ended in time t . (b) Separate contribution of each of the 100 bead long targets for the dependence of $P_{fold}(t)$ on $\log(t)$ [23].

Figure 2. Evidence for single exponential folding kinetics for chain length $N = 48$. The correlation coefficient between the logarithmic fraction of unfolded chains and ‘reaction’ time is $r \approx 0.97$ for target T4 and $r \approx 0.99$ for the remaining targets.

Figure 3. Dependence of the logarithmic folding times, $\ln_e t$, on the contact order parameter ($r \approx 0.82$).

Figure 4. Contact maps of targets T1 (a), T2 (b) and T3 (c). Each square represents a native contact. We divide the 57 native contacts into two classes: LR contacts are represented by filled squares and correspond to contacts between beads for which the backbone separation is 10 or more backbone units. Local contacts are represented by white squares. There are 23 LR contacts in structure T1, 21 in structure T2 and 44 in structure T3.

Figure 5. The backbone frequency, $\langle \omega_{|i-j|} \rangle$, as a function of the backbone separation for the low-CO, high-CO and intermediate-CO target. The backbone frequency is the mean value of $\langle \omega \rangle$ averaged over the number of contacts in each interval of backbone separation.

Figure 6. Dependence of the logarithmic folding time $\log_{10} t$ on the parameter sigma. The parameter σ varies from 0 (only local contacts contribute to the total energy) to 1 (only LR contacts contribute to the total energy).

TABLES

TABLE I: The averaged contact time, $\ln_e \langle t_0 \rangle$, as a function of the backbone separation [27]

Target	backbone distance							
	[3, 8[[8, 13[[13, 18[[18, 23[[23, 28[[28, 33[[33, 38[[38, 43[
<i>T1</i>	8.14 ± 0.12	10.67 ± 0.21	11.47 ± 0.07	11.69 ± 0.13	11.39 ± 0.07	-	11.58 ± 0.10	-
<i>T3</i>	7.66 ± 0.10	11.14 ± 0.18	10.88 ± 0.10	11.60 ± 0.06	12.06 ± 0.05	12.24 ± 0.08	11.82 ± 0.05	11.61 ± 0.05